



HAL
open science

The active fault system of SW Alps

Guillaume Sanchez, Yann Rolland, Dimitri Schreiber, Gérard Giannerini,
Michel Corsini, Jean-Marc Lardeaux

► **To cite this version:**

Guillaume Sanchez, Yann Rolland, Dimitri Schreiber, Gérard Giannerini, Michel Corsini, et al.. The active fault system of SW Alps. *Journal of Geodynamics*, 2010, 49 (5), pp.296. 10.1016/j.jog.2009.11.009 . hal-00618186

HAL Id: hal-00618186

<https://hal.science/hal-00618186>

Submitted on 1 Sep 2011

HAL is a multi-disciplinary open access archive for the deposit and dissemination of scientific research documents, whether they are published or not. The documents may come from teaching and research institutions in France or abroad, or from public or private research centers.

L'archive ouverte pluridisciplinaire **HAL**, est destinée au dépôt et à la diffusion de documents scientifiques de niveau recherche, publiés ou non, émanant des établissements d'enseignement et de recherche français ou étrangers, des laboratoires publics ou privés.

Accepted Manuscript

Title: The active fault system of SW Alps

Authors: Guillaume Sanchez, Yann Rolland, Dimitri Schreiber, Gérard Giannerini, Michel Corsini, Jean-Marc Lardeaux



PII: S0264-3707(09)00165-3
DOI: doi:10.1016/j.jog.2009.11.009
Reference: GEOD 958

To appear in: *Journal of Geodynamics*

Received date: 4-9-2009
Revised date: 17-11-2009
Accepted date: 19-11-2009

Please cite this article as: Sanchez, G., Rolland, Y., The active fault system of SW Alps, *Journal of Geodynamics* (2008), doi:10.1016/j.jog.2009.11.009

This is a PDF file of an unedited manuscript that has been accepted for publication. As a service to our customers we are providing this early version of the manuscript. The manuscript will undergo copyediting, typesetting, and review of the resulting proof before it is published in its final form. Please note that during the production process errors may be discovered which could affect the content, and all legal disclaimers that apply to the journal pertain.

The active fault system of SW Alps

Guillaume Sanchez^{1*}, Yann Rolland¹, Dimitri Schreiber¹, Gérard Giannerini¹, Michel Corsini¹, Jean-Marc Lardeaux¹.

¹Géosciences Azur UMR 6526 and Université de Nice Sophia Antipolis (UNS), CNRS and IRD, 28 Av de Valrose, BP 2135, 06108 Nice, France.

*Corresponding author. Tel: +033 492 07 68 05; fax: +033 492 07 68 16

Email addresses : Guillaume.Sanchez@unice.fr (G. Sanchez), yrolland@unice.fr (Y. Rolland), dimitri.schreiber@unice.fr (D. Schreiber) ; Gerard.GIANNERINI@unice.fr (G. Giannerini) Corsini@unice.fr (M. Corsini), lardeaux@wanadoo.fr (J.M Lardeaux).

Abstract

Historical and active seismicity in the south-western Alps (France and Italy) shows the recurrence of relatively high magnitude earthquakes ($M \geq 5.8$), like the one that recently affected the Italian Apennine range ($M=6.3$ on the 30th March 2009). However, up-to-date detailed mapping of the active fault network has been poorly established. The evaluation of seismological hazard in particular in the highly populated French and Italian coastal region cannot be done without this. Here, we present a detailed study of the main active fault system, based on geological observations along the south-western flank of the Alpine arc. This N140° right-lateral strike-slip active fault system runs along the edge of the Argentera-Mercantour range and can be followed down to the Mediterranean Sea. It is evidenced by (1) Holocene offsets of glacial geomorphology witnessing ongoing fault activity since 10 ka, (2) widespread recent (10-20 Ma) pseudotachylytes featuring long term activity of the faults, (3) active landslides along the main fault zone, (4) geothermal anomalies (hot springs) emerging in the active faults, (5) ongoing low-magnitude seismic activity and (6) localization of the main historical events. In the light of our investigations, we propose a new tectonic pattern for the active fault system in the south-western Alps.

Key words: Active fault, historical seismicity, neotectonics, seismic hazard, SW Alps.

31 1. Introduction

32 The greatest seismic hazard in France is located at the transition between the south-western
33 Alps and the Ligurian basin (Ritz et al., 1992; Sébrier et al., 1997; Eva & Solarino, 1998;
34 Baroux et al., 2001; Larroque et al., 2001; Terrier, 2006). However, the active fault network
35 sparking off the regional seismic activity is not clearly identified. Thus, the (mapping)
36 definition of active fault systems is crucial and requires detailed structural and chronologic
37 analysis.

38 The active fault system in the south-western Alps is largely controlled by inherited alpine
39 faults. Indeed, alpine tectonic displacements within the south-alpine N140°E dextral and
40 N90°E thrust fault network were established on syn-kinematic phyllosilicates by the single-
41 grain $^{40}\text{Ar}/^{39}\text{Ar}$ laser method (Corsini et al., 2004 ; Sanchez et al., 2009a ; Simon-Labric et al.,
42 2009).

43 A first set of thrust motions with “top-towards west” kinematics is recognized at ~33-34 Ma
44 and is related to burial of the European plate below the Penninic Frontal Thrust (PFT) and the
45 orogenic wedge of the Internal Alps (Fig.1; Simon-Labric et al., 2009).

46 Further, right-lateral strike-slip displacements were initiated at ~26 Ma (Corsini et al., 2004)
47 and followed at 20-22 Ma (Sanchez et al., 2009a) witnessing the onset of transcurrent motions
48 accommodated by N140 trending faults in response to sub-meridian shortening in the south-
49 western Alps. These dated shear zones were formed at mid crustal depths ($5 < P < 7$ kb – 15-
50 20 km), at temperature conditions of $350 \pm 50^\circ\text{C}$ (Sanchez et al., 2009a), at the front of the
51 mantle wedge indenter of the Ivrea Body, which is located underneath the internal Alpine
52 zone, north of the surface trace of the Penninic Frontal Thrust (Roure et al., 1996; Paul et al.,
53 2001; Bethoux et al., 2007; Schreiber et al., 2008).

54 From Middle Miocene to Pliocene, these N140°E dextral strike-slip faults were connected
55 to a sub-meridian extensional High Durance fault system and the N140°E dextral Serenne

56 fault at the south-eastern boundary of the Pelvoux massif (Tricart et al., 1996; Sue and Tricart,
57 2003) (Fig.1).

58 In this study, we focus on the south-western slope of the Argentera-Mercantour massif
59 where we have observed recent reactivation of the N140 right-lateral faults.

60

61 **2. Field investigations**

62 A field transect was performed along the major active N140E regional fault (the Tinée
63 Fault; Fig.1; Fig. 2a) on which evident geological markers have witnessed recent activity.
64 This fault is characterised by horizontal striae (Fig. 2b) and featured by significant fracturing
65 with N-S vertical joints spaced of 20-40 cm (Fig. 2c). Some of these joints are filled by
66 pseudotachylytes (detailed in Fig. 2d-h) which are connected to the fault plan showing dextral
67 movement (Horizontal striae and tension gash “en echelon”; Fig. 2b,g). As widely evoked, the
68 presence of pseudotachylytes related to fault zone records fossil earthquakes which nucleate
69 at the base of brittle seismogenic zone (<10-15km; Lin et al., 2005; Sibson and Toy, 2006). In
70 our case, this corresponds to a temperature $< 200 \pm 100^{\circ}\text{C}$ from the present-day Alpine
71 geotherm (Crouzet et al., 1999) and allows estimating the exhumation age of this deep part of
72 the seismogenic zone between 10 and 20 Ma according to fission track dates (Bigot et al.,
73 2006). This age range shows that the Tinée N140° dextral fault is active between 10 and 20
74 Ma as also suggested by the brecciation and offset of the joints observed in several places,
75 which show late deformation in relation to seismic activity (Fig. 2i).

76 Ongoing activity of this fault is also shown by the most recent Holocene slip events inferred
77 from the offset of geomorphological features (Fig. 3). Aerial photographs and field
78 investigation of the Argentera-Mercantour massif reveal a consistent 50 m dextral offset of
79 crests and glacially polished surfaces, nearby the pseudotachylyte zone (Fig.2a; Fig. 3a,b).
80 Further north in Le Pra area, along the Tinée fault, Sanchez et al. (2009b) reported similar
81 geomorphological observations. Glacially polished bedrock outcrops dated around 12 ka are

82 offset by up to 15m by some of the Tinée active fault scarps dated at 8-11 ka (Sanchez et al.,
83 2009b). Moreover, in the neighbouring La Clapière and Le Pra landslides located along the
84 Tinée active fault (Fig. 1; Fig. 2a), are dated between 10, 7 and 5 ka (Bigot et al., 2005;
85 Sanchez et et al., 2009b). Therefore, According to the damaged zone near the Tinée fault,
86 featured by a dense network of opened fractures (Fig. 3c), it is obvious that such
87 displacements can only be related to seismic activity. Moreover, in the le Pra area, we can
88 state that the 15m right-lateral offset could result from a series of post-glacial seismic events
89 post-dating 12 ka.

90

91 **3. Interpretation-Discussion**

92 *3.1 Active faults in SW Alps*

93 These structural and geochronological investigations have provided evidence for the active
94 character of the studied south-western Alps strike-slip system and allow the construction of a
95 new regional map of active faults, presented in Fig. 1. The observed morphological offsets are
96 in lateral continuation to the active Jausiers fault, whose N140°E orientation is defined by the
97 alignment of epicentres determined after the 2004-2006 seismic crisis (Fig.4; Jenatton et al.,
98 2007). The studied active fault is defined by ongoing low-magnitude seismic activity
99 represented by more than 16,000 earthquakes of maximum magnitude $M_L=2.7$ during this
100 two year period (see Figs 2b and 6 in Jenatton et al., 2007). The seismic activity was clustered
101 along a 9 km long and 3 to 8 km-deep rupture zone trending in a 140°E direction (Fig.4).
102 From focal mechanism analysis, fault motion is right-lateral strike-slip; more than half focal
103 solutions show a strike-slip motion with a NW-SE dextral plane. Only a third is extensional
104 with tension axes (T) trending NE-SW to E-W. These seismological data agree with field
105 observations at the surface, showing the two different fault trends in the NW Argentera-
106 Mercantour (Fig. 1). Inversion of fault-striae data measured in the field to determine the
107 paleo-stress directions gave similar solutions in the same zone (Fig. 4). Two main tensors

108 were obtained. The first one is featured by horizontal strike slip along the N140° faults while
109 the second one shows E-W extension along the N-S normal faults. Both are in agreement with
110 a sub-meridian shortening. A third intermediate tensor is also obtained in the transition zones
111 between the two fault types (Fig. 4). Therefore, field analysis and focal mechanisms show that
112 the Jausiers and Tinée faults correspond to a single structure hereafter called the Jausiers-
113 Tinée Fault (JTF). At a larger scale, this active fault network is outlined by numerous focal
114 mechanisms showing strike-slip and normal solutions (Delacou et al., 2004; Béthoux et al.,
115 2007). We ascribe the bimodality of focal mechanisms and paleo-stress inversions as the
116 expression of a “pull-apart” system (Fig.1; Fig.5). Following this interpretation, E-W
117 extension (Sue and Tricart, 2003; Sue et al., 2007) and 140°E right-lateral motion are
118 reconciled within a single model.

119 By analogy, at the south-eastern boundary of the Argentera-Mercantour massif,
120 instrumental seismicity is recorded along-side of the Saorge-Taggia Fault (STF) (Madeddu et
121 al., 1997), which is parallel to the JTF. The focal mechanism solutions indicate dextral strike-
122 slip motion of the STF with a N140° trending plane (Madeddu et al., 1997) in agreement with
123 the JTF geometry and kinematics. The south-eastern part of the STF active fault merges into
124 the Mediterranean (Ligurian) Sea near San Remo where the morphology of the Messinian
125 surface is strongly offset by this fault (Bigot et al., 2004).

126 Regarding the JTF and STF, seismic activity has been reported since the 16th century, with
127 earthquakes producing epicentral intensities > VIII, MSK (Sisfrance, 2008). The strongest
128 events were located near the village of La Bollène-Vésubie (AD 1564 event). It destroyed
129 most villages in the Vésubie and upper Roya Valleys and was estimated to have had a
130 magnitude of ~ 5.8 (Fig.1; Cadiot, 1979). Its localization (Cadiot, 1979; Sisfrance, 2008) near
131 the JTF (Fig. 1) allows us to attribute this event to JTF motion. Other major historical events
132 occurred near San Remo and Menton including the 1887 earthquake, which reached intensity
133 IX MSK (Sisfrance, 2008).

134 Thus, according to field investigations, seismological data and historical seismicity, it
135 appears that the STF and the JTF represent an active “en echelon” faults system (JTF-STF),
136 which localises most of the deformation in the area and on which high-magnitude earthquakes
137 ($M > 6$) may occur.

138

139 At a regional scale, moderate but regular seismicity has also been recorded along the $N20^\circ$
140 sinistral Middle Durance Fault (MDF; Cushing et al., 2008) on which five significant seismic
141 events with intensity $MSK \geq VIII$ occurred during these five last centuries (Sisfrance, 2008).
142 The MDF is linked to the “Grand Vallon and Pont de Fossé-Eychauda” fault (GVF-PFEF),
143 extending northwards into the Pelvoux massif, along which microseismicity has been
144 measured (Terrier, 2006). These observations show that the MDF-GVF-PFEF comprises a
145 unique $N20^\circ$ tectonic structure that branches into the main active fault system at the boundary
146 between the internal and external Alps. Similarly, instrumental seismicity has revealed
147 activity on other $N20^\circ$ sinistral faults, such as the Peille-Laguët (PLF; Courboulex et al.,
148 2003), Vésubie (VF) and Rouaine (RF) faults (Terrier, 2006), which are truncated by the
149 $N140^\circ$ JTF-STF (Fig.1). Deformation of Plio-Quaternary alluvial deposits has been described
150 along the Digne (Jorda et al., 1992; Hippolyte et al., 2000) and Mont Férion (Campredon et
151 al., 1977; Dubar et al., 1992) thrust, also demonstrating their recent reactivation with a dextral
152 strike-slip component (Bès-MontDenier Fault: BMDF; St Blaise-Aspremont fault: BAF; Fig.
153 1).

154 Thus, the tectonic framework of the south-western external Alps exhibits a conjugate active
155 fault system formed by $N140^\circ$ dextral and $N20^\circ$ sinistral faults compatible with a sub-meridian
156 shortening context (Fig.1).

157

158 *3.2 Seismic hazard evaluation*

159 These new findings have implications for the evaluation of seismological and related
160 (landslide, tsunami) hazards in one of the most populated regions of the Mediterranean Sea
161 coast (the Riviera). Seismicity reported on the JTF-STF during the last decade is moderate
162 ($M < 4$) and the historical earthquake catalogue (Sisfrance, 2008) does not report any
163 significant event along the entire fault. However, the offset of topographic crests and glacial
164 morphology observed along the JTF-STF imply a major paleoseismic event. As many authors
165 have pointed out, different slips and stress drops can be observed from large earthquakes with
166 similar sizes (Wells and Coppersmith, 1994; B. Romanowicz and Ruff, 2002; Manighetti et
167 al., 2007). In particular, Manighetti et al. (2007) claimed that such variability of slips could be
168 related to the fault geometry. Indeed, a segmented fault, breaking in shorter but more strongly
169 energetic ruptures, may display higher slip than an un-segmented fault. Along the extremely
170 segmented JTF-STF system, the maximum displacement observed (15m and 50m), can lead
171 to magnitude overestimation with respect to a more mature un-segmented fault. Therefore, the
172 offset morphologies could result from the recurrence of lower magnitude earthquakes ($M \approx 6$)
173 and creeping processes also cannot be ruled out. In the same way, the seismic potential of the
174 MDF-GV-PFEF, which corresponds to the major N20 conjugate fault, has been assessed by
175 palaeoseismological investigations that suggest the possibility of a strong earthquake between
176 27 and 9 ka (Sébrier et al., 1997). Concerning the seismic hazard related to the N20
177 conjugated faults (RF, VF and PLF), the present-day seismicity remains lower than the main
178 N140E fault system, even if nothing proves that a large earthquake along these minor faults
179 could not occur though it is suggested by the AD 1618 and AD 1664 earthquakes (Sisfrance,
180 2008). Thus, more work has to be done to estimate the motions on these smaller fault
181 segments as they merge into the densely populated coastal zone. Even lower magnitude
182 earthquakes ($M \leq 6$) on these minor faults could cause dramatic damage given their shallow
183 hypocenter depth and local site effects.

184

185 **4. Conclusions**

186 Based on field investigations and seismicity, it is concluded that the south-western Alps has
187 been subject to transcurrent deformations since at least the Holocene period, mainly
188 accommodated by a > 100 km long, N140°E dextral segmented active fault system (JTF-
189 STF), a conjugate N20 sinistral fault (MDF GV-PFEF) and minor conjugate N20 sinistral
190 (RF, VF, PLF) and N-S extensional (HDF) or dextral faults (DF, BAF, BF, SF). These active
191 faults share some general characteristics of intraplate faults, such as their relatively slow
192 tectonic motions. Infrequent but large earthquakes ($M \approx 6$) may be expected near the densely
193 populated French and Italian coastlines but the recurrence and magnitude of such events
194 remains to be estimated.

195

196 **Acknowledgments**

197 This work was part of the GIS-CURARE regional project to analyse the geohazards in the
198 Alpes-Maritimes. We thank P. Tricart and one anonymous reviewer for their constructive
199 remarks.

200

201 **References**

- 202 Angelier, J., 1990. Inversion of field data in fault tectonics to obtain the regional stress—III.
203 A new rapid direct inversion method by analytical means. *Geophysical Journal*
204 *International* 103, 363–376.
- 205 Baroux, E., Béthoux, N. and Bellier, O., 2001. Analyses of the stress field in southeastern
206 France from earthquake focal mechanisms. *Geophysical Journal International* 145,
207 336-348.
- 208 Béthoux, N. Sue, C., Paul, A., Virieux, J., Fréchet, J., Thouvenot, F., Cattaneo, M., 2007.
209 Local tomography and focal mechanisms in the south-western Alps: Comparison of
210 methods and tectonic implications. *Tectonophysics* 432(1-4), 1-19.

- 211 Bigot-Cormier, F., Braucher, R., Bourles, D., Guglielmi, Y., Dubar, M., Stephan, J.-F., 2005.
212 Chronological constraints on processes leading to large active landslides. *Earth and*
213 *Planetary Science Letters* 235(1-2), 141-150.
- 214 Bigot-Cormier, F., Sage, F., Sosson, M., Deverchere, J., Ferrandini, M., Guennoc, P., Popoff,
215 M., Stephan, J.F., 2004. Pliocene deformation of the north-Ligurian margin (France) :
216 consequences of a south-Alpine crustal thrust. *Bulletin de la Société Géologique de*
217 *France* 175(2), 197-211.
- 218 Bigot-Cormier, F., Sosson, M., Poupeau, G., Stéphan, J.F., Labrin, E., 2006. The denudation
219 history of the Argentera Alpine External Crystalline Massif (Western Alps, France-
220 Italy): an overview from the analysis of fission tracks in apatites and zircons.
221 *Geodinamica Acta* 19/6, 455-473.
- 222 Cadiot, B., 1979. Le séisme Nissart de 1564. Mémoire n°96: BRGM, France.
- 223 Campredon, R., Franco, M., Giannerini, G., Gigot, P., Irr, F., Lanteaume, M., Spini, H.,
224 Tapoul, J-F., 1977. Les déformations de conglomérats pliocènes de l'arc de nice
225 (Chaînes subalpines méridionales). *Comptes Rendus sommaires de la Société*
226 *Géologiques de France* 2, 75-77.
- 227 Corsini, M., Ruffet, G., Caby, R., 2004. Alpine and late hercynian geochronological
228 constraints in the Argentera Massif (Western Alps). *Eclogae Geologicae Helvetiae* 97, 3-
229 15.
- 230 Courboux, F., Larroque, C., Deschamps, A., Gélis, C., Charreau, J., Stéphan, J.F., 2003. An
231 unknown active fault revealed by microseismicity in the south-east of France.
232 *Geophysical Research Letters* 30.
- 233 Crouzet, C., Menard, G., Rochette, P., 1999. High-precision three-dimensional
234 paleothermometry derived from paleomagnetic data in an Alpine metamorphic unit.
235 *Geology* 27(6), 503-506.

- 236 Cushing, E.M. Bellier, O., Nechtschein, S., Sébrier, M., Lomax, A., Volant, Ph., Dervin, P.,
237 Guignard, P., Bove, L., 2008. A multidisciplinary study of a slow-slipping fault for
238 seismic hazard assessment: the example of the Middle Durance Fault (SE France).
239 *Geophysical Journal International* 172(3), 1163-1178.
- 240 Delacou, B., Sue, C., Champagnac, J.D., Burkhard, M., 2004. Present-day geodynamics in the
241 bend of the western and central Alps as constrained by earthquake analysis.
242 *Geophysical Journal International* 158(2), 753-774.
- 243 Dubar, M., Guglielmi, Y., Falgueres, C., 1992. Néotectonique et sédimentation cotière
244 quaternaires en bordure de l'arc subalpin de Nice (A.M., France). *Quaternaire* 3, 105-
245 110.
- 246 Eva, E., Solarino, S., 1998. Variations of stress directions in the western Alpine arc.
247 *Geophysical Journal International* 135, 438-448.
- 248 Hippolyte, J.C., Dumont, T., 2000. Identification of Quaternary thrusts, folds and faults in a
249 low seismicity area: examples in the Southern Alps (France). *Terra Nova* 12(4), 156-
250 162.
- 251 Jenatton, L., Guiguet, R., Thouvenot, F., Daix, N., 2007. The 16,000 event 2003-2004
252 earthquake swarm in Ubaye (French Alps). *Journal of Geophysical Research*, 112.
- 253 Jomard, H., Lebourg, T., Binet, S., Tric, E., Hernandez, M., 2007. Characterization of an
254 internal slope movement structure by hydrogeophysical surveying. *Terra Nova* 19(1),
255 48-57.
- 256 Larroque, C. Béthoux, N., Calais, E., Courboulex, F., Deschamps, A., Déverchère, J.,
257 Stéphan, J.F., Ritz, J.F., Gilli, E., 2001. Active deformation at the junction between
258 southern French Alps and Ligurian basin. *Netherlands Journal of Geosciences* 80,
259 255-272.
- 260 Lin, A. Maruyama, T., Stallard, A., Michibayashi, K., Camacho, A., Kano, K., 2005.
261 Propagation of seismic slip from brittle to ductile crust: evidence from

- 262 pseudotachylyte of the Woodroffe thrust, central Australia. *Tectonophysics* 402, 221-
263 35.
- 264 Madeddu, B., Béthoux, N., Stéphan, J.F., 1997. Champ de contrainte post-pliocène et
265 deformations récents dans les Alpes sud-occidentales. *Bulletin de la Société*
266 *Géologique de France* 167, 797-810.
- 267 Manighetti, I., Campillo, M., Bouley, S., Cotton, F., 2007. Earthquake scaling, fault
268 segmentation, and structural maturity. *Earth and Planetary Science Letters* 253(3-4),
269 429-438.
- 270 Paul, A., Cattaneo, M., Thouvenot, F., Spallarossa, D., Béthoux, N., Fréchet, J., 2001. A three-
271 dimensional crustal velocity model of the southwestern Alps from local earthquake
272 tomography. *Journal of Geophysical Research* 106.
- 273 Ritz, J.-F., 1992. Tectonique récente et sismotectonique des Alpes du Sud : analyses en
274 termes de contraintes. *Quaternaire* 3, 111-124.
- 275 Romanowicz, B., Ruff, L.J., 2002. On moment-length scaling of large strike slip earthquakes
276 and the strength of faults. *Geophysical Research Letters* 29, C6136382H1400A1011-
277 9F8RH647.
- 278 Roure, F., Choukroune, P., Polino, R., 1996. Deep seismic reflection data and new insights on
279 the bulk geometry of mountain ranges. *Comptes Rendus d'Académie des Sciences de*
280 *Paris* 322(2a), 345-359.
- 281 Sanchez, G., Rolland, Y., Corsini, M., Jolivet, M., Bricchau, S., Olliot, E., Goncalves, P.,
282 2009a. Exhumation along transpressive dextral strike slip fault in the Argentera massif
283 (south-western Alps) constrained by structural, metamorphism and low-temperature
284 thermochronology. *Geophysical Research Abstracts*, 11.
- 285 Sanchez, G., Rolland, Y., Corsini, M., Braucher, R., Bourlès, D., Arnold, M., Aumâtre, G.,
286 2009b. Relationships between tectonics, slope instabilities and climate changes:

- 287 Cosmic ray exposure dating of active faults and landslides in the SW Alps.
288 Geomorphology, doi:10.1016/j.geomorph.2009.10.019.
- 289 Schreiber, D. Lardeaux, J.M, Courrioux, G., Martelet, G., Guillen, A., 2008. 3D modelling of
290 alpine Mohos in south-western Alps. International Geological Congress Abstracts.
291 Congres Geologique International, Resumes, 33.
- 292 Sébrier, M., Ghafiri, A., Bles, J.-L., 1997. Paleoseismicity in France: Fault trench studies in a
293 region of moderate seismicity. *Journal of Geodynamics* 24(1-4), 207-217.
- 294 Sibson, R.H. and Toy, V.G., 2006. The habitat of fault-generated pseudotachylite: presence
295 versus absence of friction melt. In: Abercrombie, R.E., McGarr, A., Di Toro, G. and
296 Kanamori, H. (eds) *Earthquakes: Radiated Energy and the Physics of Faulting*.
297 Geophysical monograph, American Geophysical Union 170, 153-166.
- 298 Simon-Labric, T. Rolland, Y., Dumont, T., Heymes, T., Authemayou, C., Corsini, M.,
299 Fornari, M., 2009. ⁴⁰Ar/³⁹Ar dating of Penninic Front tectonic displacement (W
300 Alps) during the Lower Oligocene (31-34 Ma). *Terra Nova* 21(2), 127-136.
- 301 SisFrance, 2008. Catalogue de la sismicité historique de la France. BRGM/EDF/IRSN,
302 <http://www.sisfrance.net>.
- 303 Sue, C. Delacou, B., Champagnac, J.D., Allanic, C., Tricart, P., Burkhard, M., 2007.
304 Extensional neotectonics around the bend of the Western/Central Alps: an overview.
305 *International Journal of Earth Sciences* 96(6), 1101-1129.
- 306 Sue, C., Tricart, P., 2003. Neogene to ongoing normal faulting in the inner western Alps: a
307 major evolution of the late alpine tectonics. *Tectonics* 22 (5), 1-25.
- 308 Terrier, M., 2006. Identification et hiérarchisation des failles actives de la Région Provence-
309 Alpes-Côte d'Azur. BRGM/RP-53930-FR.
- 310 Tricart, P., Bouillin, J.P., Dick, P., Moutier, L., Xing, C., 1996. Le faisceau de failles de
311 haute-Durance et le jeu distensif du front Briançonnais au SE du Pelvoux (Alpes
312 occidentales) = The High Durance Fault-Zone and the extensional reactivation of the

313 Briançonnais Front Thrust, to the SE of the Pelvoux Massif (Western Alps). Comptes
 314 rendus de l'Académie des sciences. Série 2. Sciences de la terre et des planètes 323(3),
 315 251-257.

316 Wells, D.L., Coppersmith, K.J., 1994. New empirical relationships among magnitude, rupture
 317 length, rupture width, rupture area, and surface displacement. Bulletin of the
 318 Seismological Society of America 84(4), 974-1002.

319
 320

321 **Figure caption**

322 Fig. 1. Regional geological map of the active fault network in the south-western Alps
 323 (Hautes-Alpes to Alpes Maritimes, France), with the locations of key geological markers
 324 including faults, landslides (Jomard et al., 2007) and geothermal anomalies. Location of the
 325 AD 1564 historical seismic event is also shown. Focal mechanisms along the main fault have
 326 been taken from Courboux et al. (2003), Delacou et al. (2004) and Bethoux et al. (2007).
 327 The size represents the magnitude. PFT: Penninic Frontal Thrust; DCFT: Digne-Castellane
 328 Frontal Thrust, CT; Castellane Thrust; NT: Nice Thrust; JF: Jausier fault; TF: Tinée fault;
 329 STF: Saorge-Taggia fault; PLF: Peille-Laghet fault; VF: Vésubie fault; BAF: St Blaise-
 330 Aspremont fault; RF: Rouaine fault; BMDF: Bès-MontDenier fault; MDF: Middle Durance
 331 fault; GVF: Grand-Vallon fault; PFEF: Pont de Fossé-Eychauda fault; HDF: High Durance
 332 fault; SF: Serenne fault; BF: Bersézio fault.

333

334 Fig. 2. Pictures of field relationships in the Argentera-Mercantour crystalline massif
 335 (orthogneiss) along the Tinée Fault zone transect. a. General view of Clapière landscape
 336 showing the Tinée fault zone; b. Evidence of right-lateral motion along the Tinée fault with
 337 horizontal striae and schistosity deflection. c. Regularly spaced N-S joints in the damage zone
 338 along the Tinée fault. d,e. Pseudotachylyte veins infilling the N-S joints. f. Pseudotachylyte

339 joints containing pure quartz clasts and showing cataclastic features evolving locally to
340 ductile stretching of clasts in the central part of the joints. g. Tension gash “en echelon” filled
341 by pseudotachylytes showing dextral movement of the Tinée fault. h. Pseudotachylyte joints
342 reaching several centimetres in width. i. Brecciation and offset of pseudotachylyte joints.

343

344 Fig. 3. Pictures showing evidence of right-lateral displacement of the ≥ 10 ka
345 geomorphology. a, aerial photograph, with the main fault underlined in black; offset
346 geomorphological markers include offset crests (✱) and slope break (●). b, landscape
347 photograph showing the same markers. c, damaged zone along the fault located on b, featured
348 by numerous cracks and fractures with a high angle to the fault strike.

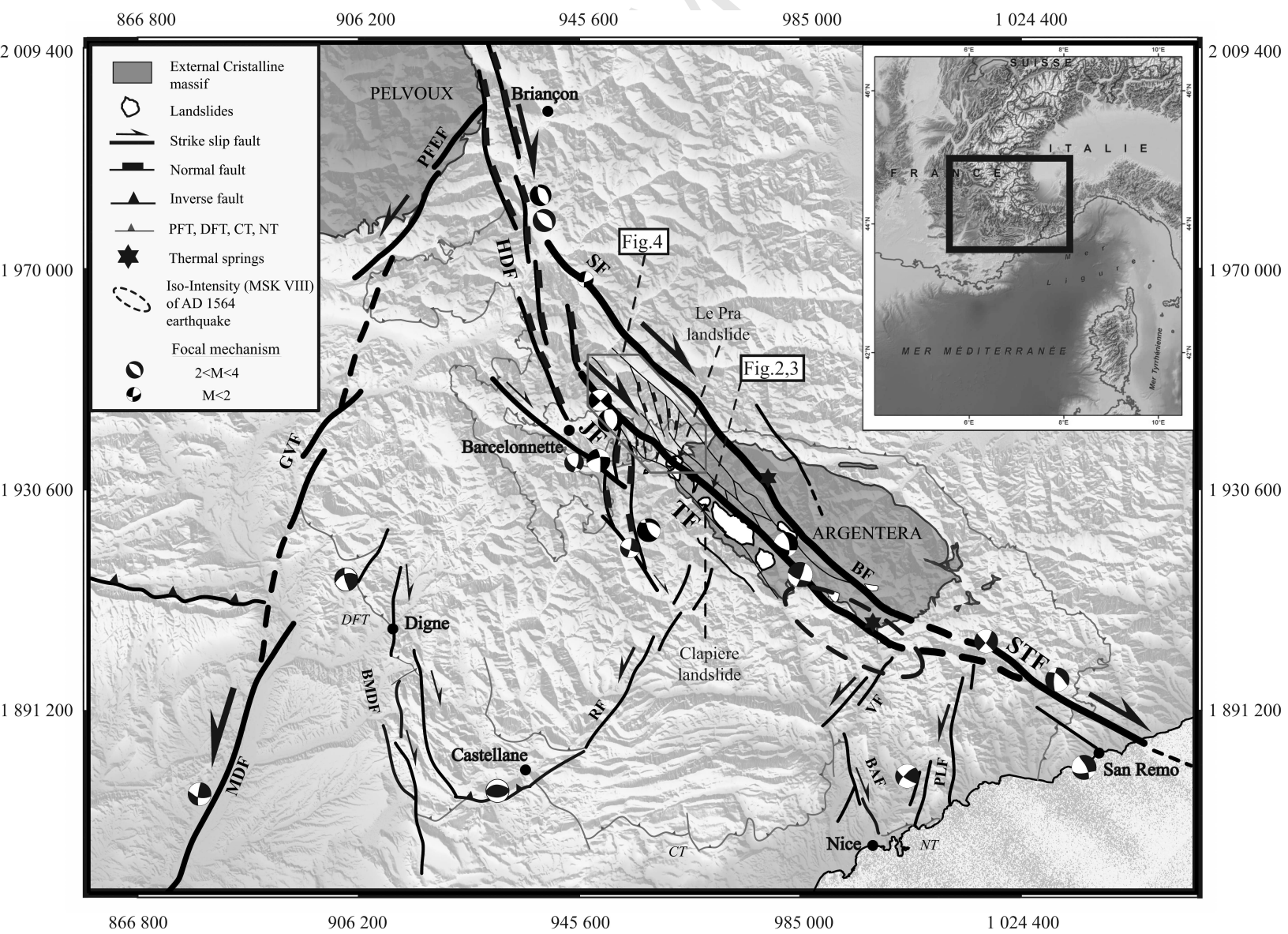
349

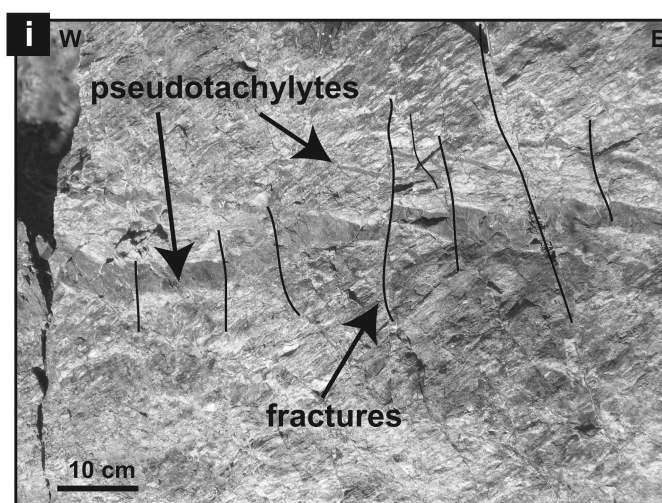
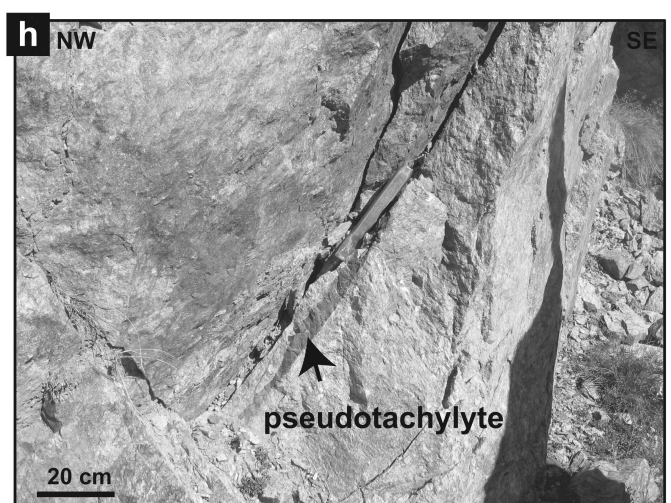
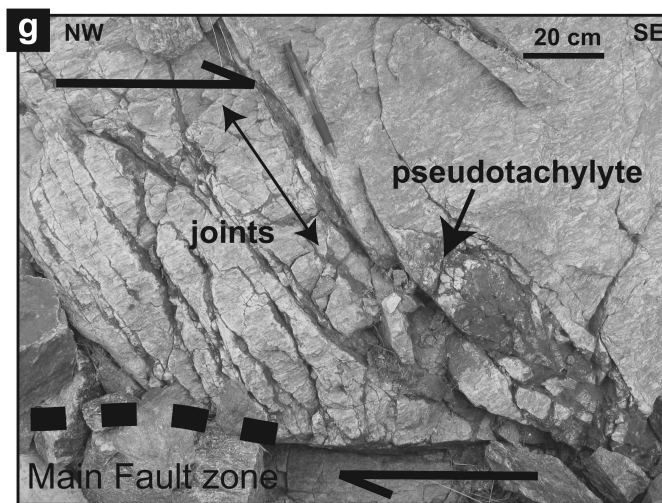
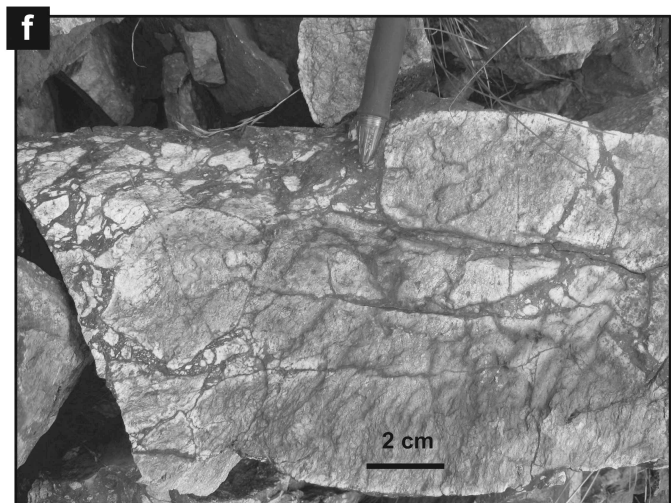
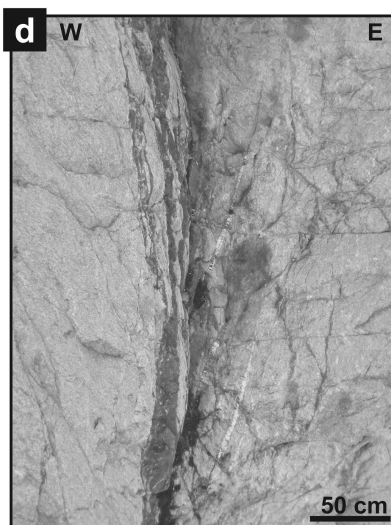
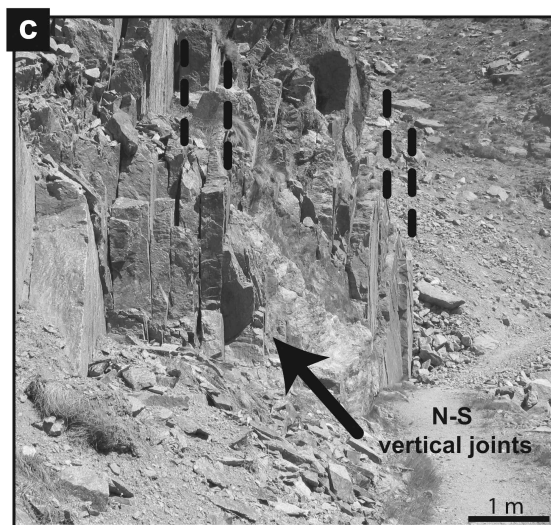
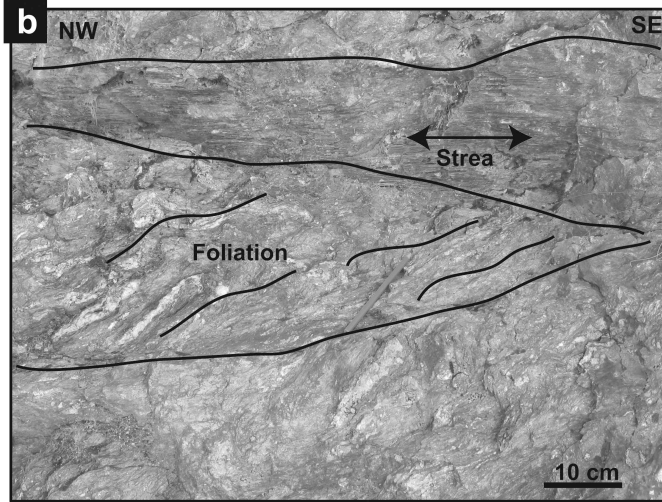
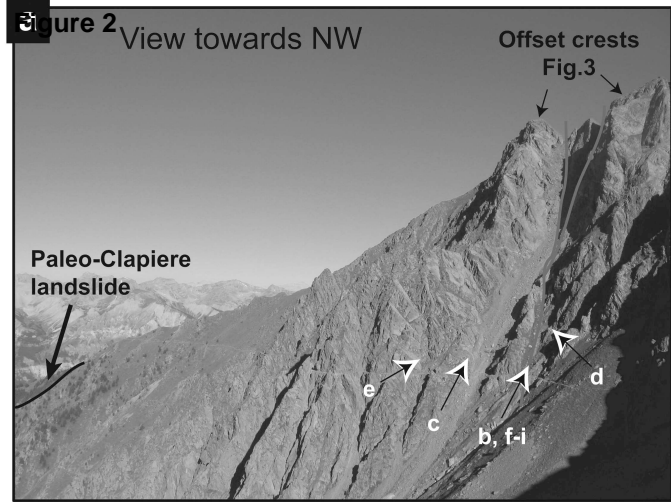
350 Fig. 4. Relationship between focal mechanisms and paleostress axes along the JTF. The
351 cartographic data correspond to field investigations locally filled out by 1/50 000 geological
352 maps data. Focal mechanisms along the Jausier fault (JF) have been taken from Jenatton et al.
353 (2007). Schmidt stereonet in lower hemisphere showing the distribution of more than 70
354 measured fault and striae and the computation of paleostress axes determined with Tector
355 software (Angelier, 1990). Stars with 5,4,3 branches mark the principal stress axes of σ_1 , σ_2
356 and σ_3 respectively. Large grey arrows show directions of compression and extension with
357 azimuthal confidence in grey. The contours around poles give the principal stress axes
358 uncertainty during the inversion.

359 Fig. 5. Block diagram showing the active fault system in the north-western part of the south-
360 western Alps. The picture represents the pull-apart system with the two major dextral Jausier-
361 Tinée fault and Serennes-Bersézio fault and the extensional High Durance fault system.

362

363





Script

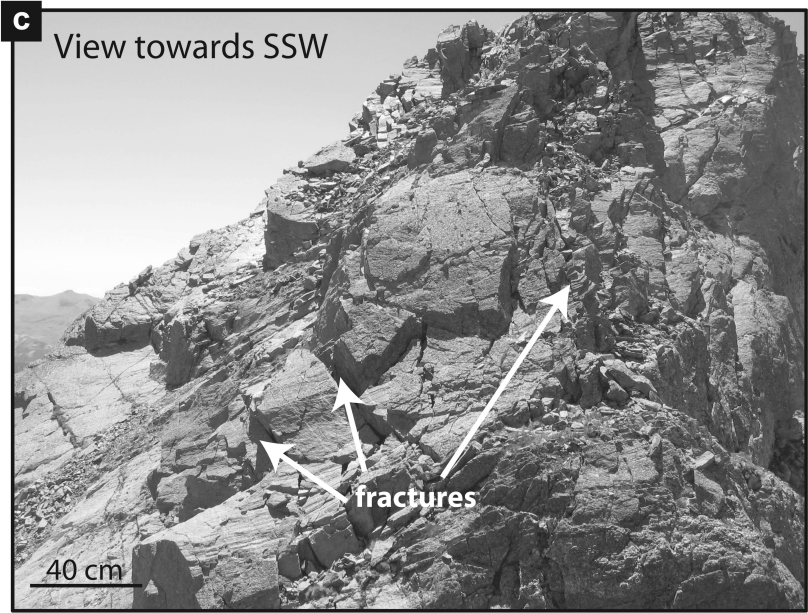
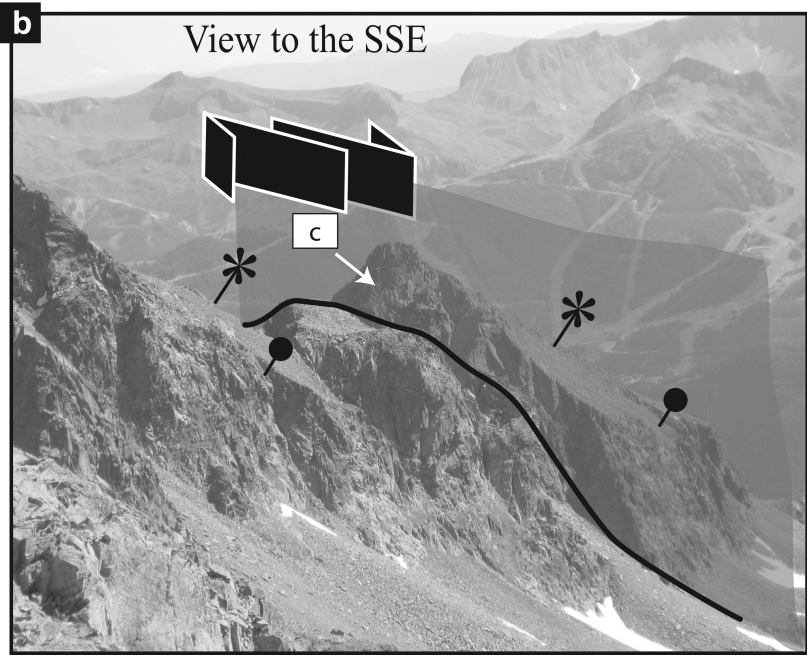
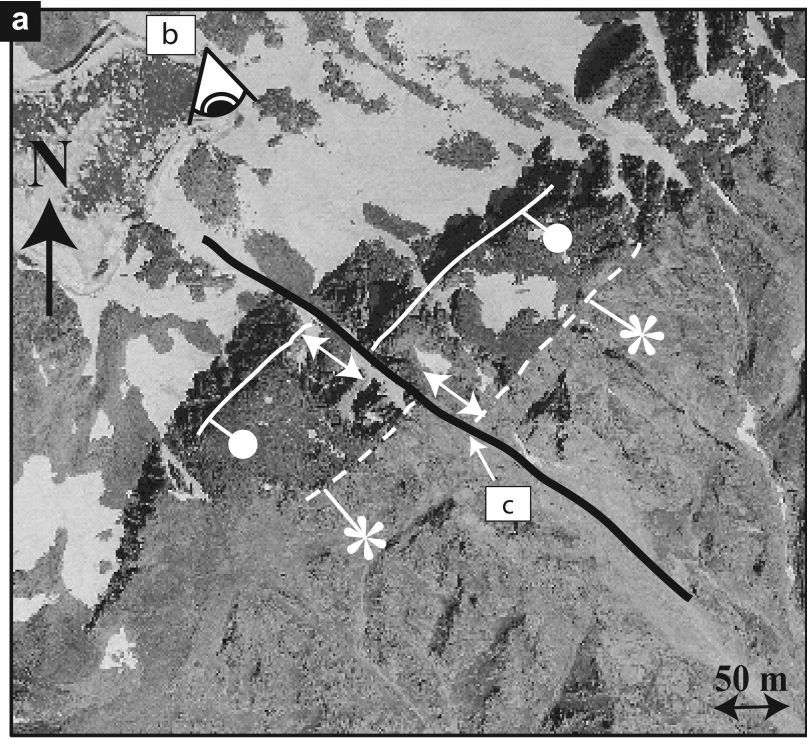
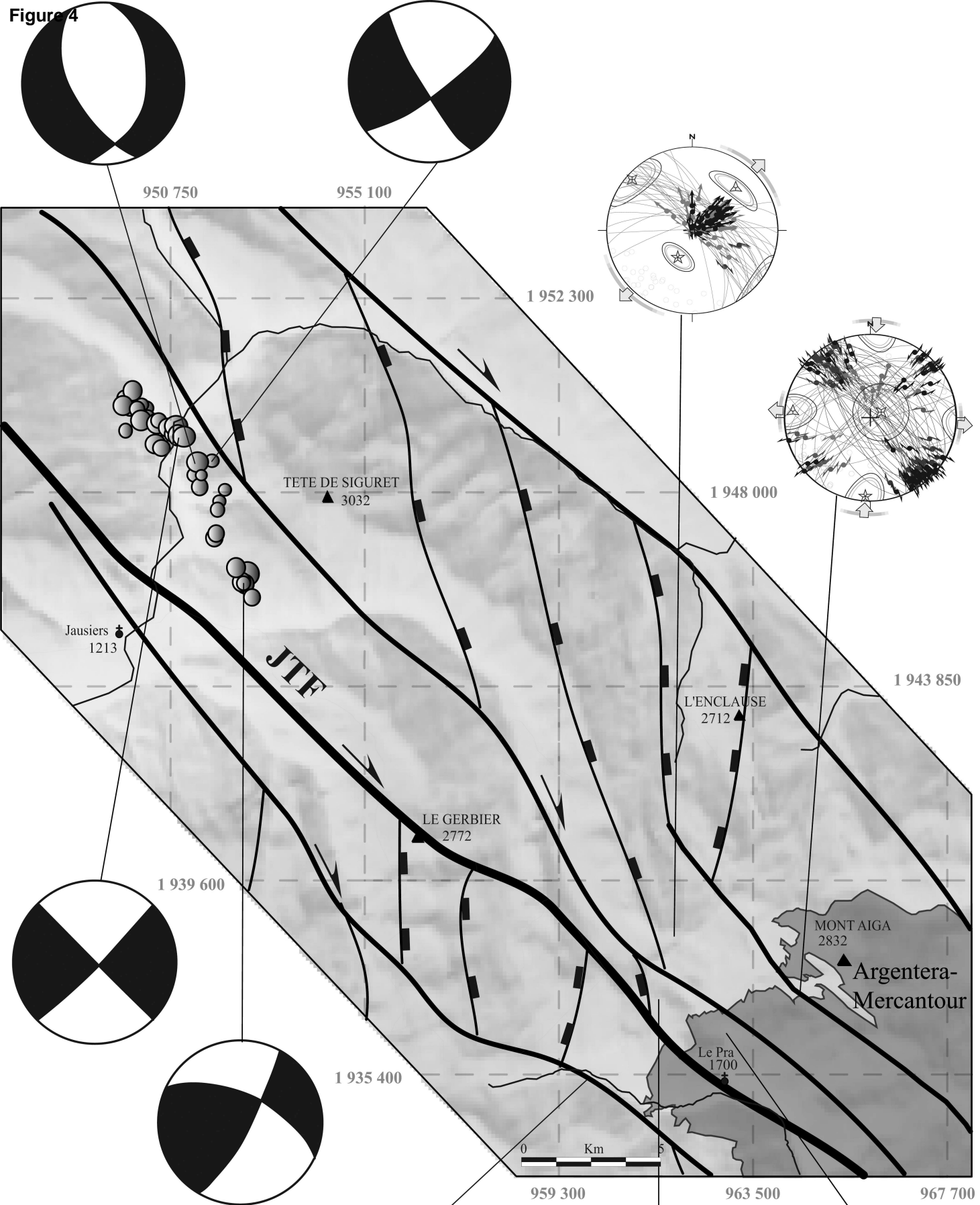









Figure 4



-  External Cristalline massif
-  Strike slip fault
-  Normal fault
-  Epicentral location of earthquake
-  σ_1
-  σ_2
-  σ_3

